Int J Adv Manuf Technol (2014) 71:263–277
DOI 10.1007/s00170-013-5465-0

ORIGINAL ARTICLE

Processing parameters affecting cold spay coatings performances

P. Cavaliere · A. Silvello

Received: 6 March 2013 / Accepted: 24 October 2013 / Published online: 24 November 2013

Abstract In the present paper, the microstructural and mechanical properties of metal–metal cold spray deposits are described. Different spray particles coatings (Al-, Ti-, Ni-based particles) deposited on different substrates (Al-, Ti-, Fe-, Ni-, Mg-based bulk materials) were produced and their mechanical and microstructural properties were characterized. Microhardness, porosity, grain size and adhesion strength of the coatings were analyzed as a function of processing parameters such as particle velocity, particle dimensions, gas density, substrate hardness, and temperature. The results were employed to build a database used to obtain a provisional model through a multi-objective optimization software. For each different substrate and particle type, the working points were defined in terms of processing parameters to optimize mechanical and microstructural behavior of coatings. The error calculation of the final properties of the deposits demonstrated the precision of the developed model.

Keywords Cold spray · Processing parameters · Optimization

1 Introduction

Cold spraying is a coating technology based on aero and high-speed impact dynamics of small particles (usually 1–50 μm in diameter). A coating is formed through the intensive plastic deformation of particles impacting on a substrate at a temperature well below the melting point of the spray material. It can be considered a safe and green technology because of the absence of a high-temperature gas jet, radiation, and explosive gases. An example of a key application of the cold spray process is the recovery of costly aircraft parts during overhaul and repair. Cold spray also can be used in the development of unique materials and for the production of actual parts. Cold spray can be used to produce a new class of materials that could not be achieved by conventional ingot metallurgy. Even if it has great application potentials in aerospace, automobile manufacture, chemical industry, etc., there are still many fundamental aspects to be uncovered. Since adhesion of the metal powder to the substrate and deposited material is achieved in the solid state, the characteristics of cold spray deposits are quite unique. Cold spray can potentially provide with restoration, sealing, surface modification, wear resistance, thermal barriers, heat dissipation, rapid prototyping, aesthetic coatings, fatigue resistance, and many other applications without the undesirable effects of process temperatures or metallurgical incompatibilities among materials. It can also be used to increase the heat resistance of a material. Research, aimed to improve the cold spraying technology, is still being conducted worldwide today. Many interesting papers have been presented in literature in the most recent years. In [1–8], there is a description of mechanical and microstructural behavior of Ti coatings on different substrates with particular emphasis on the effect of processing parameters. In [9–21], the different possibilities are shown of spraying pure Al or Al–alloys on different substrates such as Al–alloys, Mg–alloys, and steel underlying the phenomenon of severe plastic deformation of particles during impact. In [22, 23], a detailed description of Mg alloy corrosive protection through cold spray is shown. In [24–31], we find the properties of cold spray Ni, Ni-Cr and Al alloys particles on various substrates. Cu and Cu alloys deposit properties are described in [32–38]. Mechanical properties of cold spray coatings strongly depend on particles bonding on the substrate; such bonding is dependent on mechanical properties of the substrate and particles and on the processing parameters employed during spray. Some authors emphasize the

P. Cavaliere (✉) · A. Silvello
Department of Innovation Engineering, University of Salento,
via per Arnesano, 73100 Lecce, Italy
e-mail: pasquale.cavaliere@unisalento.it

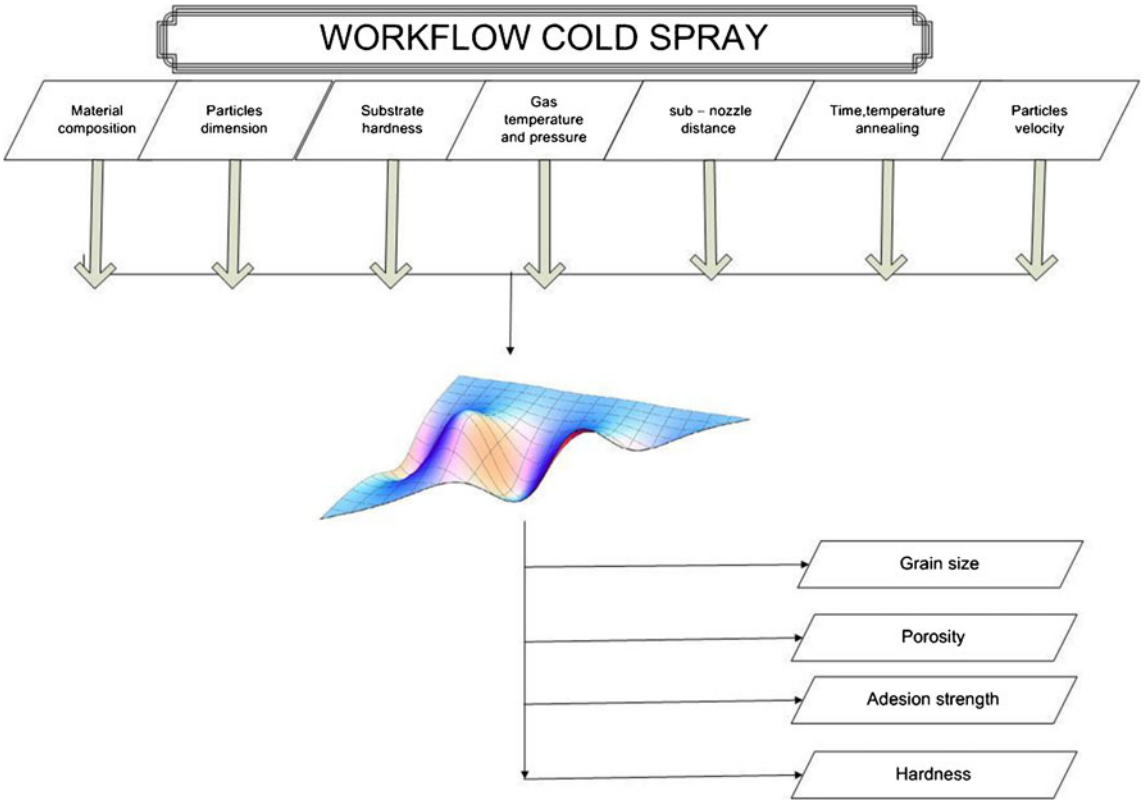

Fig. 1 Workflow of the analyses

enhancement of shear instability as an instrument to improve such bonding [28, 39], such non-equilibrium phenomena lead to the deformation inducing melting during impact which increases the bonding effect during spray clearly the phenomenon is enhanced as improving processing parameters as a function of the different materials of the substrate and particles. It has been also demonstrated that the surface finishing strongly influences the substrate deposit interface microstructure and consequently the microstructural and mechanical behavior [34]; depending on the difference between the hardness of the impacting particles and substrate, the processing parameters can lead to different aspect of the interface: interfacial instability and adiabatic shear instability [39, 40]. The conclusion is that with the same material, the processing conditions can lead to a shift between the behaviors. From an experimental point of view, it seems that the matter of fact is the incoming of partial melting due to particular localized conditions, such conclusions (supported by numerical

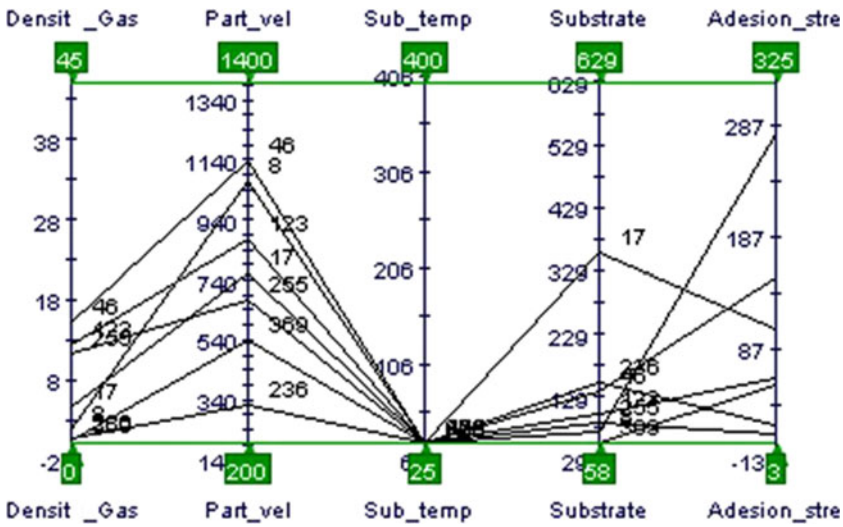

Fig. 2 Design space in terms of main input ranges, in *red* they are indicated the six validation designs

investigations) have been demonstrated for some specific materials and conditions but the results seem not conclusive at the present. Other authors focus the attention on the coupling between critical velocity of the particles and hard/soft interaction between the substrate and the particles leading to optimal conditions for metal on metal bonding [41]; in the present paper, the velocity of the particles and the difference between the hardness of the substrate and of the particles were largely considered in the analyses of the results. Flow pressure governing particles speed and gas temperature is fundamental. Flow pressure and particle speed are directly related to the impact energy. If such energy is too low, the particles do not bond to the substrate and consequently erode it. Temperature is fundamental because it regulates the particles ductility leading them to correctly flatten for bonding.

The in-depth analysis of industrial processes, depending on different parameters, needs the employment of computational multi-objective optimization tools. modeFRONTIER® (mF) platform allows the managing of a wide range of experimental data and the obtaining of an easy overview of the entire product development process. The correct employing of a design of experiment (DOE) technique leads to a reduction in the number of calculations. After that, these well-distributed results can be used to create an interpolating surface. These kinds of interpolation and regression methodologies are also known as response surface methods (RSMs). The subject of the present paper was necessary because of the large amount of processing parameters and results belonging to various particles sprayed on different substrates. By employing such technique, it can be possible to monitor the physical properties and processing parameters affecting cold spray coatings performances. In addition, the developed model provides with a useful tool to predict mechanical and microstructural features in conditions different from the ones belonging to the original database. Once data have been obtained, whether from an

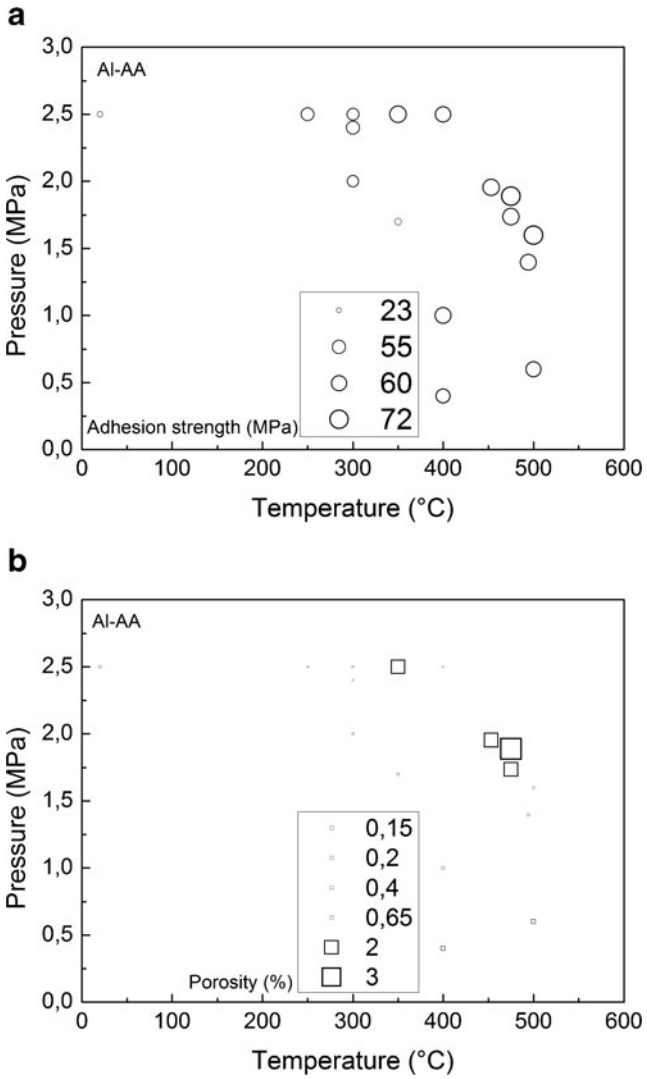

Fig. 3 Al on AA7075 adhesion strength (**a**) and porosity (**b**)

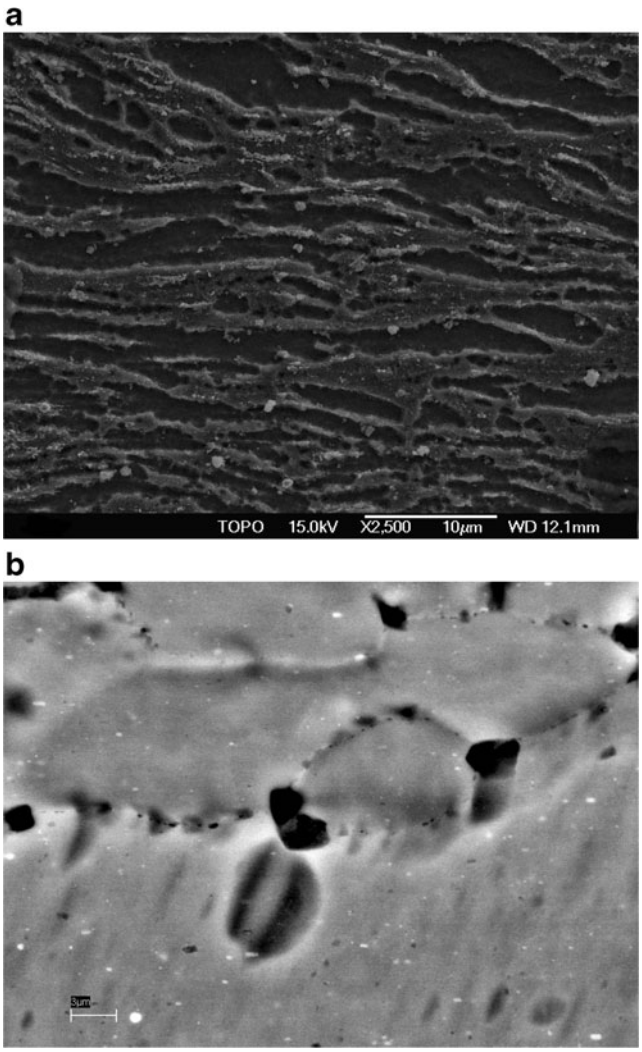

Fig. 4 Microstructure of aluminum particles sprayed on AA7075 at 500 °C and 1.5 MPa

optimization or DOE, the user can turn to the extensive post-processing features to analyze the results.

2 Experimental procedure

Different cold spray deposits were prepared by employing CGT Kinetics 4000 series Cold spray system with a tungsten carbide MOC De Laval nozzle. The deposits were prepared on different substrate materials by employing different particles characterized by various dimensions. The cold spray parameters in the present study were: substrate temperature, gas type, gas temperature and pressure, nozzle–substrate distance. The monitored outputs were: deposit grain size, micro hardness, adhesion strength, and porosity. The mean grain size of the deposits was measured through X-ray diffraction by using a Rigaku Ultima + diffractometer, selected specimens were characterized through TEM observations for measurements comparisons. The microhardness and the adhesion strength were measured by employing NanoTest MICROMATERIAL^{TM} platform. The porosity was calculated through a statistical analysis performed on Zeiss EVO40 SEM observations, for each sample five different images of 200× 200 μm^2 were analyzed. To allow modeFRONTIER to compute the effect of the gas change, the values of the different gas densities as a function of their temperature were introduced in the database. The database was built by introducing the input parameters, the corresponding output for each processing condition experimentally analyzed and the physical correlations between the different conditions. The overall process is outlined in the workflow through the analysis carried out by modeFRONTIER (Fig. 1).

3 Numerical procedure

The workflow is divided into data flow (solid line) and logic flow (dotted line) which have a common node (calculator

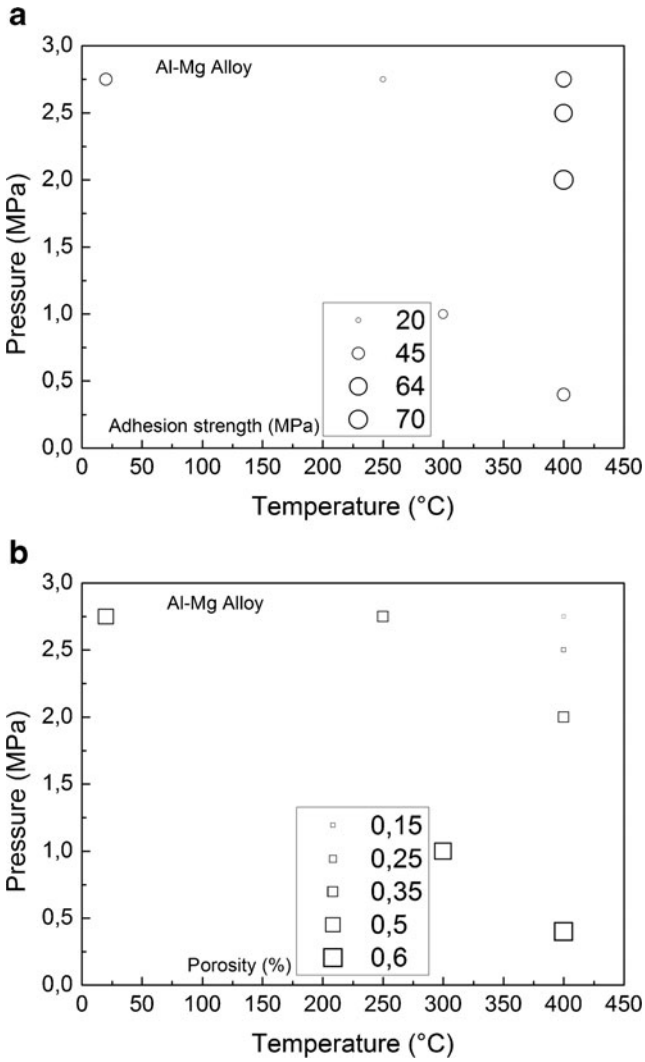

Fig. 5 Al on Mg alloy adhesion strength (**a**) and porosity (**b**)

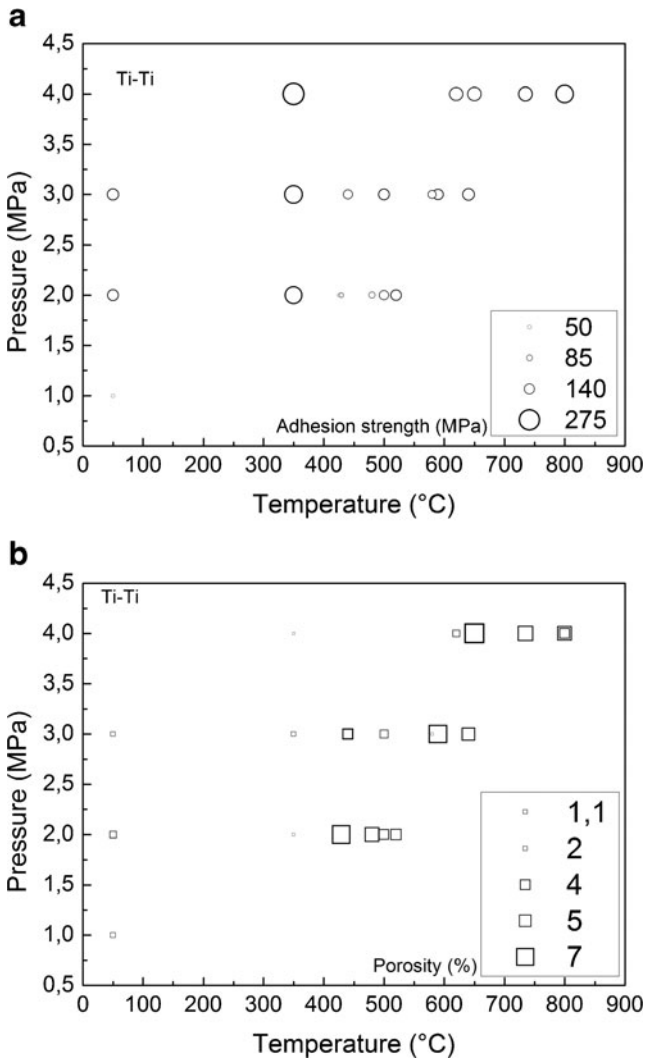

Fig. 6 Ti on pure Ti adhesion strength (**a**) and porosity (**b**)

node) in which mathematical functions, representative of the process, are introduced. In the data flow, all the parameters that should be optimized in numerical simulations are introduced: material, particle dimensions, substrate temperature, gas temperature and pressure, substrate–nozzle distance, particle velocity. The output variables define a multipurpose and have been minimized or maximized taking into account some constraints or limitations typical of the actual process. At this point, the nodes that make up the logic flow of numerical analysis are defined. The first node is the DoE, which is the set of design from which the different possible working conditions are analyzed. Therefore, it means achieving a set number of designs that will be used by the scheduler (the node where the best algorithm is introduced) for optimization. In the present case, an appropriate method of assessment proposed by the modeFRONTIER was used: reduced factorial. This method has the very important characteristic of not presenting relationships between variables, and allows us to create a space design covering all the different possible configurations and more easily achieving the optimum. The core work flow is a specific response surface, which proves to be the only node in common between the Logical flow and data flow. For each output variable to be minimized, it is necessary to create a response surface. The next step is to evaluate the performance surface and use them as a node operator in our work flow. The available tools are the ones offered by modeFRONTIER, such as RSM distance, the RSM residual, and RSM function plot. After an analysis of all, areas carried out through different tools proposed in the design space of mF panel, the optimal condition of analysis for each of the output variables can be chosen. The choices lead to the use of RBF type surfaces with the MultiQuadrics Hardy's radial function. New designs fill all the range of analysis. These designs are introduced in the response surface that has been set in the first step of study. In this way, mF generates a determined number of working parameters which lead to a particular goal. At this point the user has to choose the set of input that optimizes the value of each output, considering the physical and technological constraints. The experimental design consists of 376 input and output obtained from experimental data. To train the virtual surface in the training phase, they were included 370 experimental design input and output. The remaining six were used in the design validation phase. Such last designs were chosen in order to fulfill all the design space in terms of input ranges (Fig. 2).

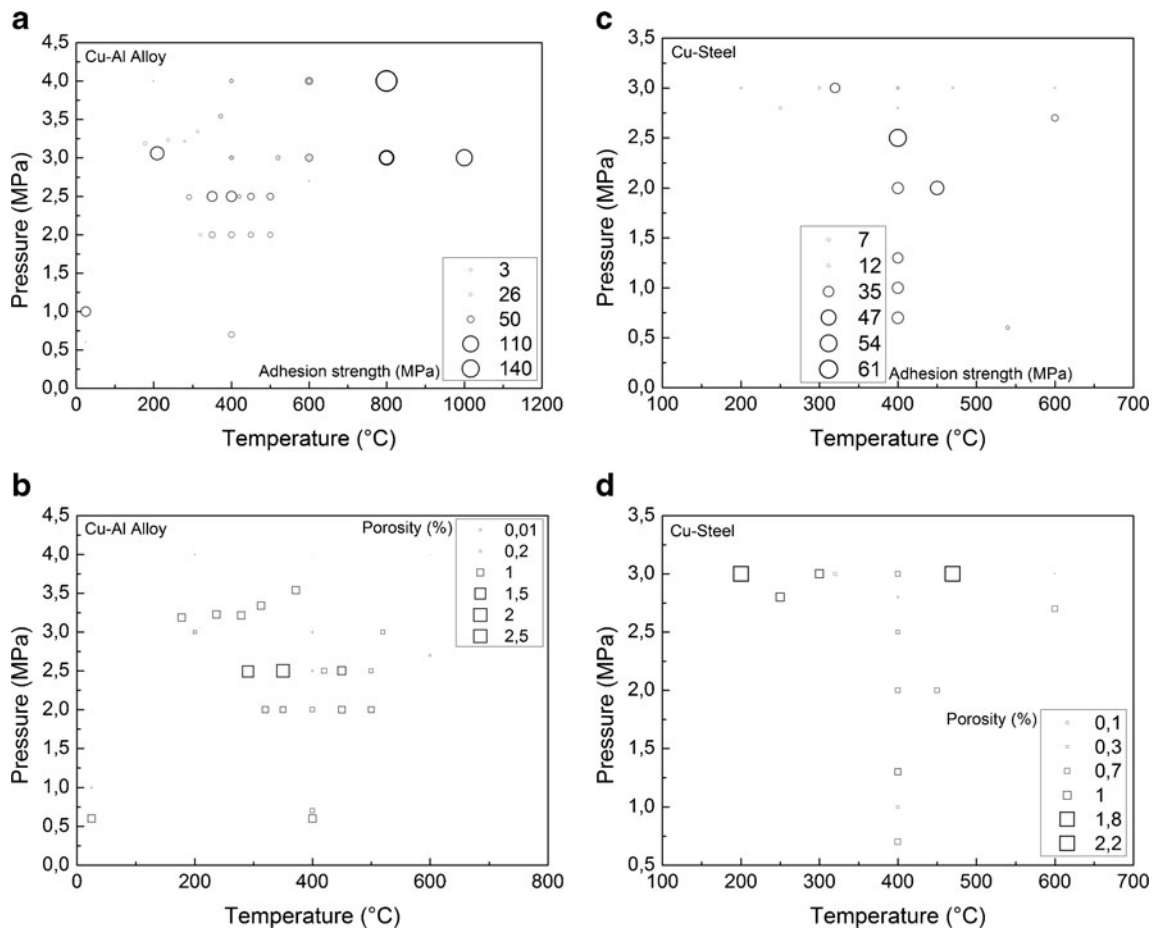

Fig. 7 Cu on AA7075 adhesion strength (**a**) and porosity (**b**). Cu on steel adhesion strength (**c**) and porosity (**d**)

In the validation phase, the Δ error was measured including in the "trained" RSM only the input remaining conditions. Then, the numerical calculated results were compared with the experimental ones.

4 Results and discussion

The results in terms of mechanical and microstructural properties of cold deposits have been analyzed as a function of the deposited materials on different substrates. The first main parameters, affecting the final properties of the deposited samples, were working gas pressure and temperature. They resulted fundamental in the variation of adhesion and porosity of the deposits. The higher the pre-heat temperature is, the higher is the thermal energy retained by the particles impacting on the substrate. The deposition of the coatings was carried out with a single step at a high transverse velocity. Thus, the gas interaction with the substrate material was limited. In terms of cold spray coatings, it is important to note that the gas temperature will increase the substrate temperature. A very different behavior was observed by changing sprayed particles and substrates. In Fig. 3, the adhesion strength and deposit porosity as a function of gas pressure and temperature in the case of aluminum particles on AA7075 substrate are shown.

The adhesion strength shows a maximum in correspondence of high gas temperature and intermediate pressure. An example of the microstructure of aluminum particles sprayed on AA7075 at 500 °C and 1.5 MPa is shown in Fig. 4.

In the same conditions, the porosity of the deposits results very high. Normally, the efficiency of the deposits in terms of porosity reduction is related to high particles deformation (related to the particles speed and pressure); such porosity is inversely proportional to the gas temperature. In fact, the higher is the temperature, the larger results the melting due to deformation that conduces to an increase in porosity also in the case of high levels of adhesion strength. In the case of pure

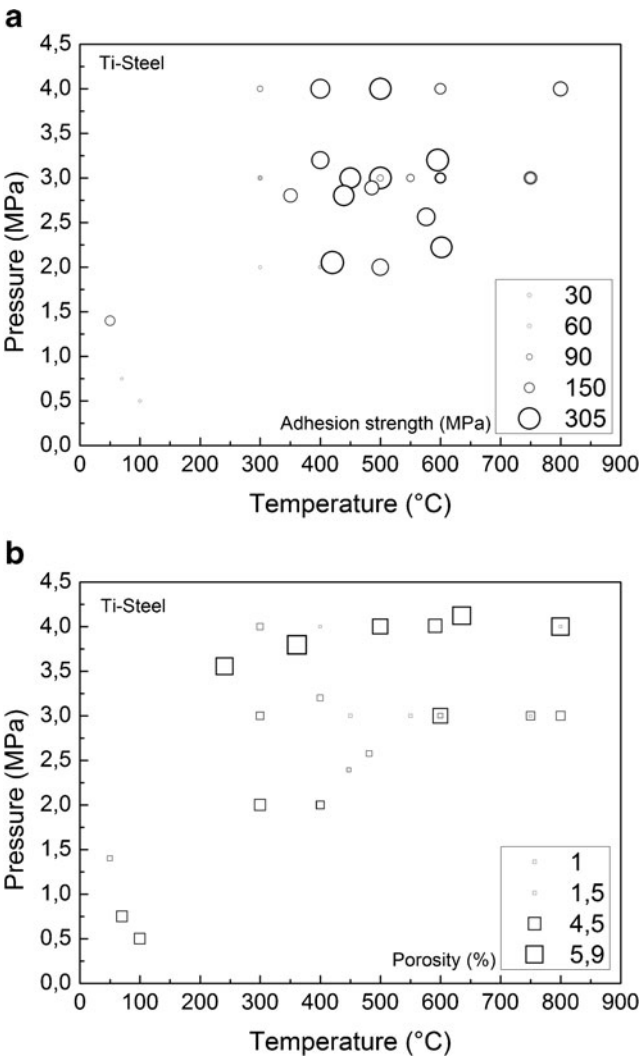

Fig. 8 Ti on steel adhesion strength (**a**) and porosity (**b**)

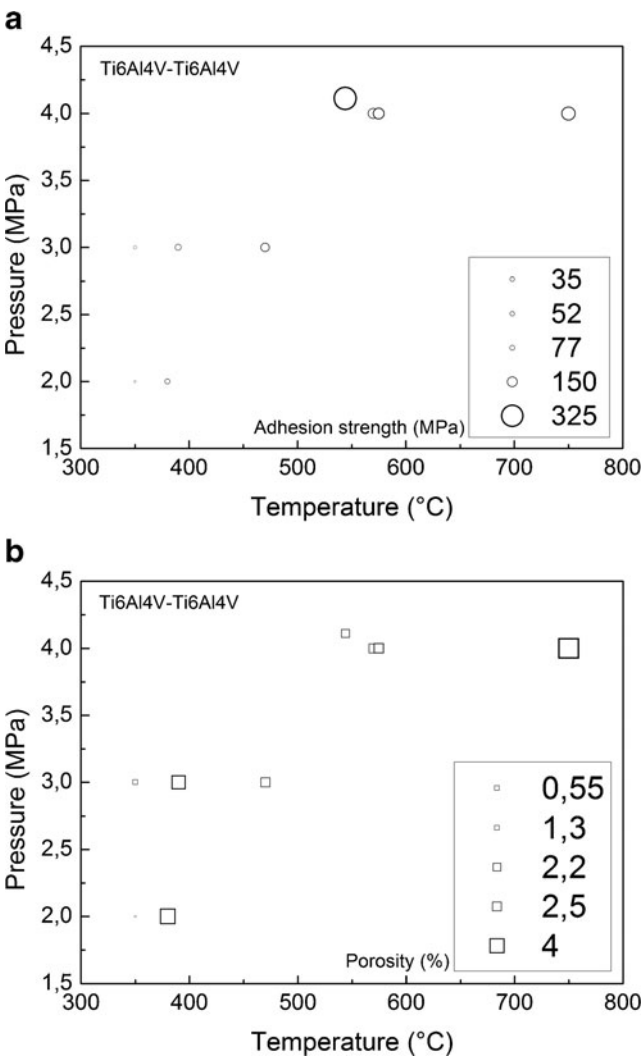

Fig. 9 Ti6Al4V on Ti6Al4V adhesion strength (**a**) and porosity (**b**)

aluminum particles, sprayed on magnesium alloys substrates, adhesion strength shows maximum values for high temperature and pressure; in such conditions, deposit porosity shows minimum levels (Fig. 5).

A similar behavior was observed for titanium particles sprayed on pure titanium substrate; in such cases, high adhesion strength is shown for high pressure and intermediate temperature (Fig. 6).

In such conditions, porosity shows the minimum level. A more energetic impact of the particles on the substrate leads to more plastic deformation; this part of the coating formation process leads to metallurgical bonding as well as porosity reduction. In such case, the processing conditions are optimal to reduce melting (Ti has a melting point very higher with respect to aluminum alloys) and to have a non-melting mediated deformation in order to reach low levels of porosity with very high levels of adhesion strength. The best coupling between high adhesion strength and low porosity is reached for temperature of 350 °C and 4 MPa of gas pressure, far from such conditions adhesion strength tends to be lower with an increase in the deposit porosity. Copper particles deposited on AA7075 show maximum values of adhesion strength in correspondence to high temperature and high pressure (Fig. 7a);

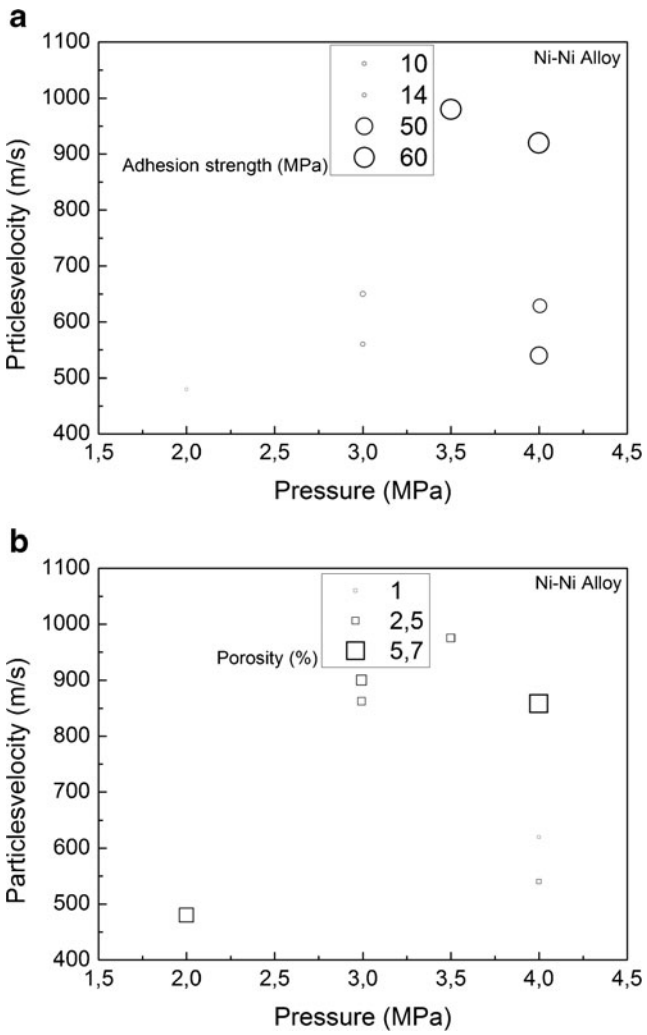

Fig. 10 Ni on Ni adhesion strength (**a**) and porosity (**b**)

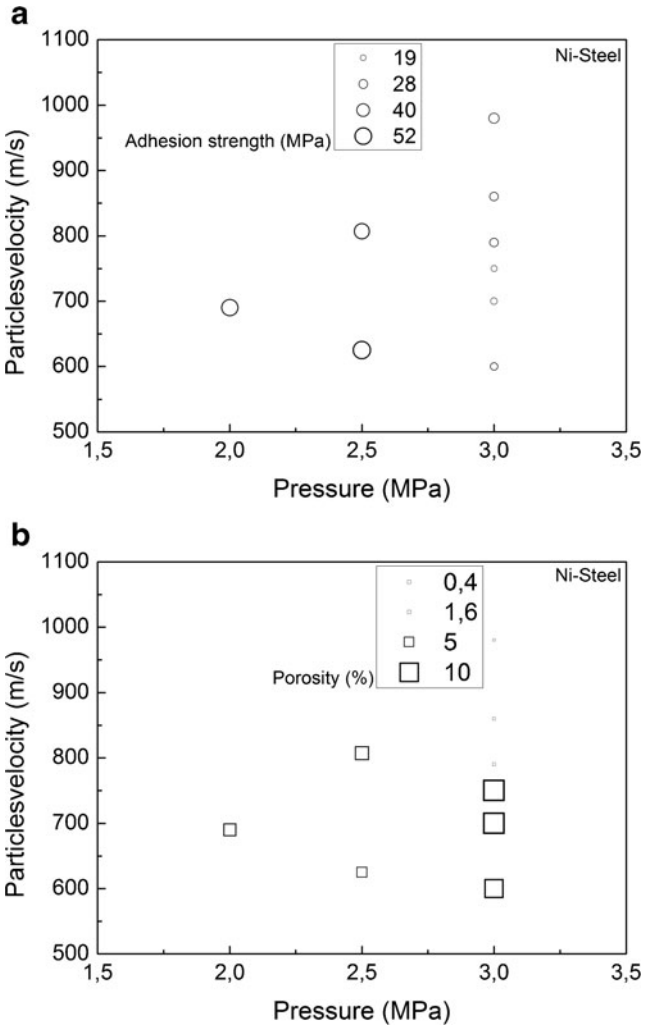

Fig. 11 Ni on steel adhesion strength (**a**) and porosity (**b**)

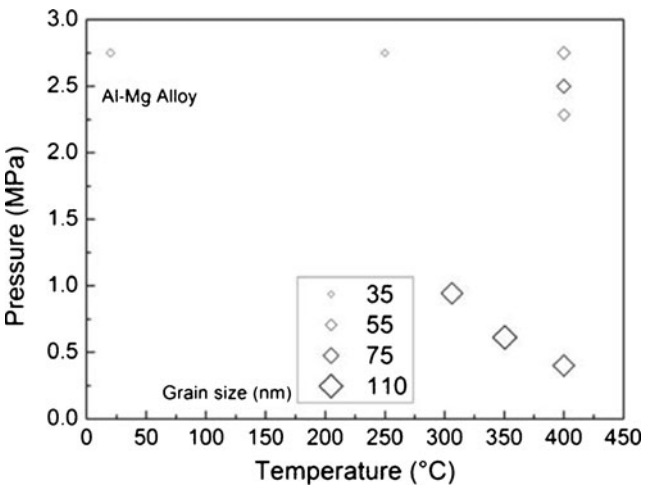

Fig. 12 Grain size variation Al deposits on AZ91

Table 1 Correlation coefficients indicating the relationships between the different input and output analyzed in the present study

	Correlation coefficients										
	Gas density	Pressure	Temperature	Distance	Velocity	Sub_Temperature	Sub_HV	Adhesion	Grain size	Dep_HV	Porosity
Gas density	1	0.675	0.062	0.415	0.102	0.12	0.073	0.037	−0.18	−0.035	0.035
Pressure	0.675	1	0.307	0.322	0.349	0.157	0.19	0.385	−0.247	0.143	0.08
Temperature	0.062	0.307	1	0.003	0.291	0.115	0.056	0.383	−0.243	0.184	0.025
Distance	0.415	0.322	0.003	1	0.182	−0.056	0.093	0.022	−0.11	0.096	0.042
Velocity	0.102	0.349	0.291	0.182	1	0	0	0.461	−0.319	0.187	−0.089
Sub_Temperature	0.12	0.157	0.115	−0.056	0	1	0.193	0.241	−0.096	0.046	0.145
Sub_HV	0.073	0.19	0.056	0.093	0	0.193	1	0.05	−0.13	0.309	0.235
Adhesion	0.037	0.385	0.383	0.022	0.461	0.241	0.05	1	−0.191	0.183	0.138
Grain size	−0.18	−0.247	−0.243	−0.11	−0.319	−0.096	−0.13	−0.191	1	−0.148	−0.016
Dep_HV	−0.035	0.143	0.184	0.096	0.187	0.046	0.309	0.183	−0.148	1	0.008
Porosity	0.035	0.08	0.025	0.042	−0.089	0.145	0.235	0.138	−0.016	0.008	1

in the same conditions, the porosity of the deposits shows minimum levels (Fig. 7b). In the case of copper deposited on steel substrate, the maximum values in adhesion strength (Fig. 7c) and the minimum levels of porosity (Fig. 7d) are reached for intermediate values of pressure and temperature.

The same behavior has been observed in the case of pure titanium deposited on steel substrate (Fig. 8).

Such behavior is due to the very similar hardness between Cu–steel and Ti–steel, resulting in a strong jetting of the particles appearing just in a very narrow range of spraying conditions. Ti6Al4V particles sprayed on Ti6Al4V substrate show the best deposition performances in correspondence of high gas pressure and intermediate temperatures (Fig. 9).

By changing process conditions, changes in the in-flight velocity of cold sprayed particles were obtained. The analysis of the deposition of Ni particles shows that such material is strongly sensitive to the particles velocity (function of the pressure), the gas temperature and the particles size; in the case of cold-sprayed Ni the analysis of the results was conducted as a function of the pressure and particles velocity.

Ni sprayed on Ni substrate shows the best performances for high gas pressure and high particles velocity (Fig. 10).

The sprayed metallic powder particles impacted onto the substrate in a solid state are heavily deformed in a very short period, typically less than 10 ns, and well bonded to the substrate. Furthermore, the severe and nearly adiabatic plastic deformation generates heating of the impacted region and forms very fine grains with the size of several tens of nanometers within the particles. It is suggested that the grain refinement results from in situ dynamic recrystallization. Actually, it seems that a higher particle velocity is necessary to make much larger plastic deformation. In the case of Ni

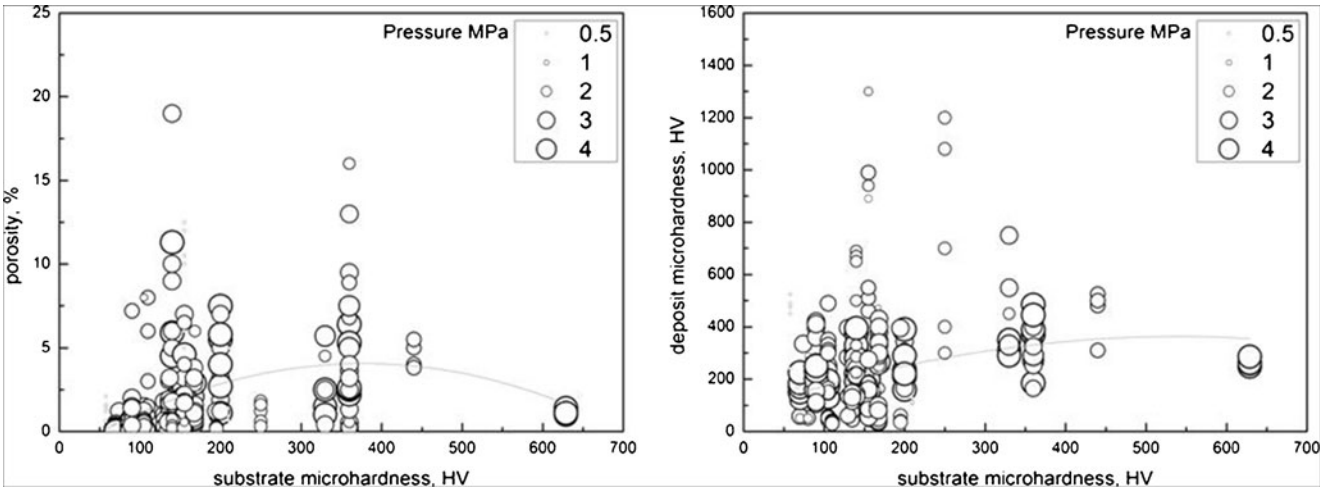

Fig. 13 Deposit porosity and microhardness as a function of gas pressure and substrate microhardness

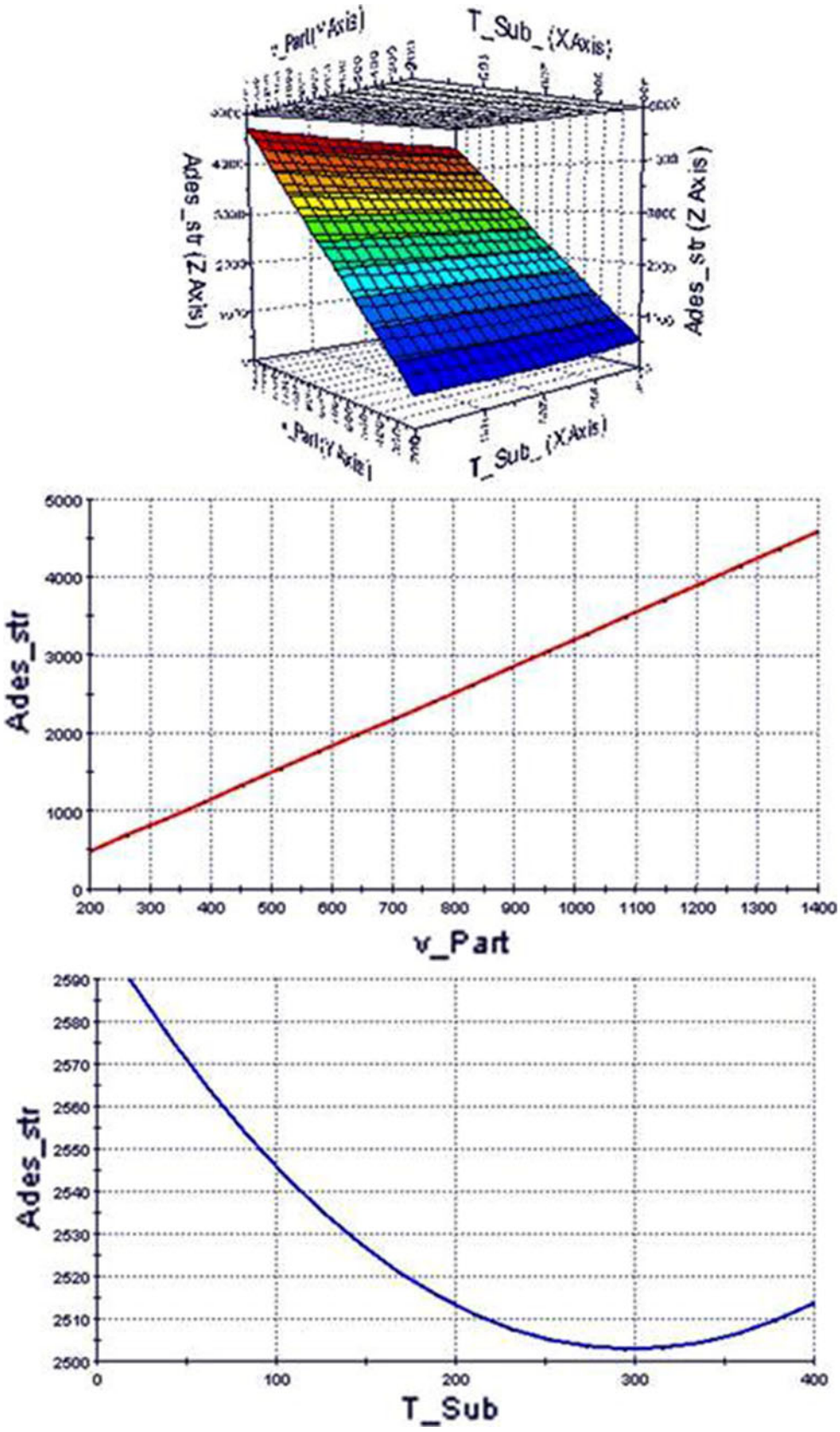

Fig. 14 Adhesion strength vs. particles velocity and substrate temperature (*Ades_str* is the adhesion strength; *T_sub* is the substrate temperature; *v_part* is the particles velocity)

particles sprayed on steel substrate, the best performances are in correspondence to intermediate values of pressure and velocity (Fig. 11).

The ability of cold-sprayed particles to undergo plastic deformation and adiabatic shear is a function of material properties, such as yield strength and melting point as well

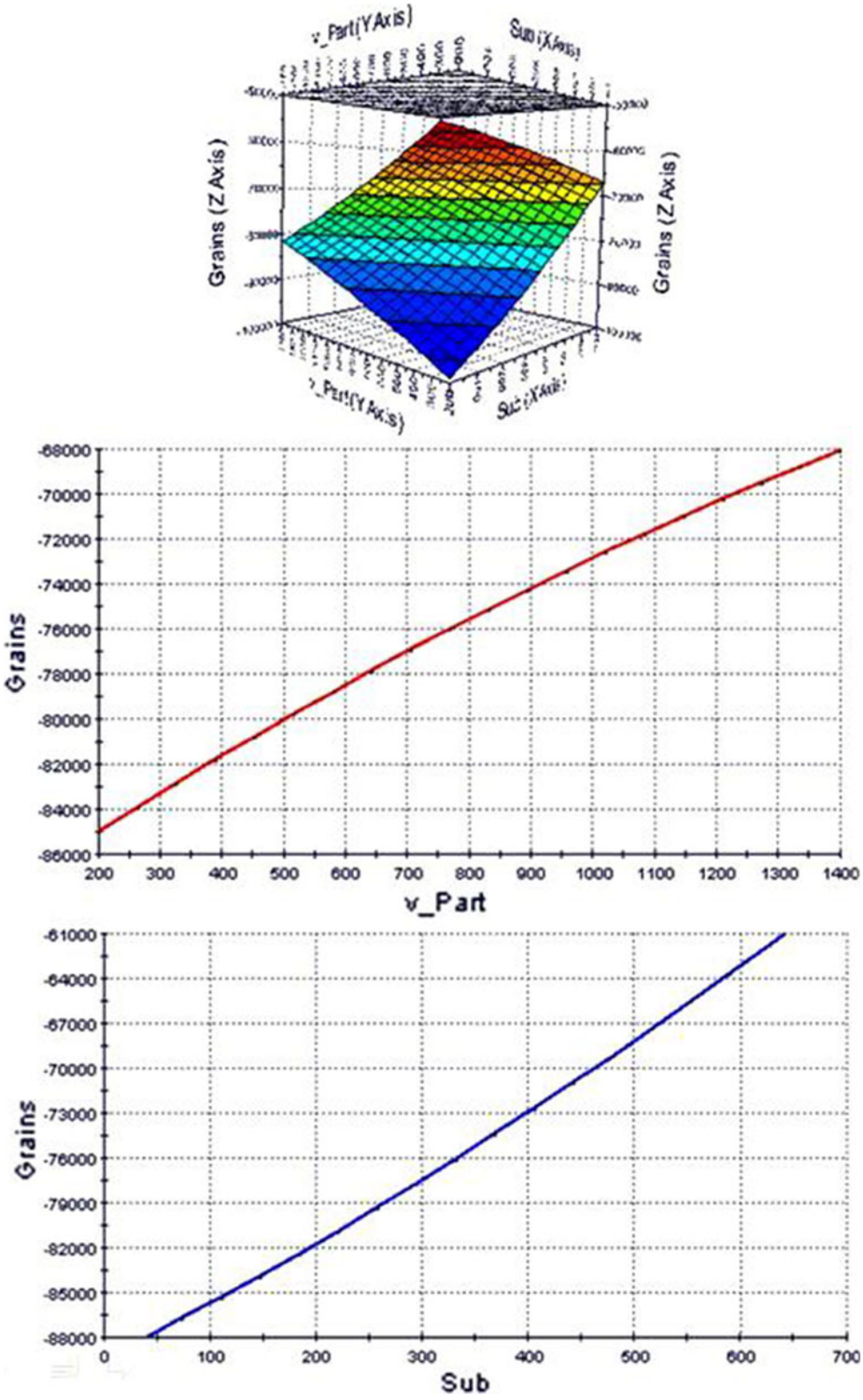

Fig. 15 Grain size vs. particles velocity and substrate hardness (*Grains* is the deposit grain size; *Sub* is the substrate hardness; *v_Part* is the particles velocity)

as process conditions, such as deposition temperature, particle velocity, and particle size. When a particle reaches the substrate at its critical velocity, adiabatic shear takes place contributing to the formation of a metallurgical bonding. For each condition of substrate, particle pressure and temperature, it is possible to individuate a critical velocity of the particles. For speeds higher than such critical velocity, bonding is not achieved. The substrate deformation contributed to the formation of an intimate, possibly metallurgical, contact between the materials. In the case of substrate much harder than the

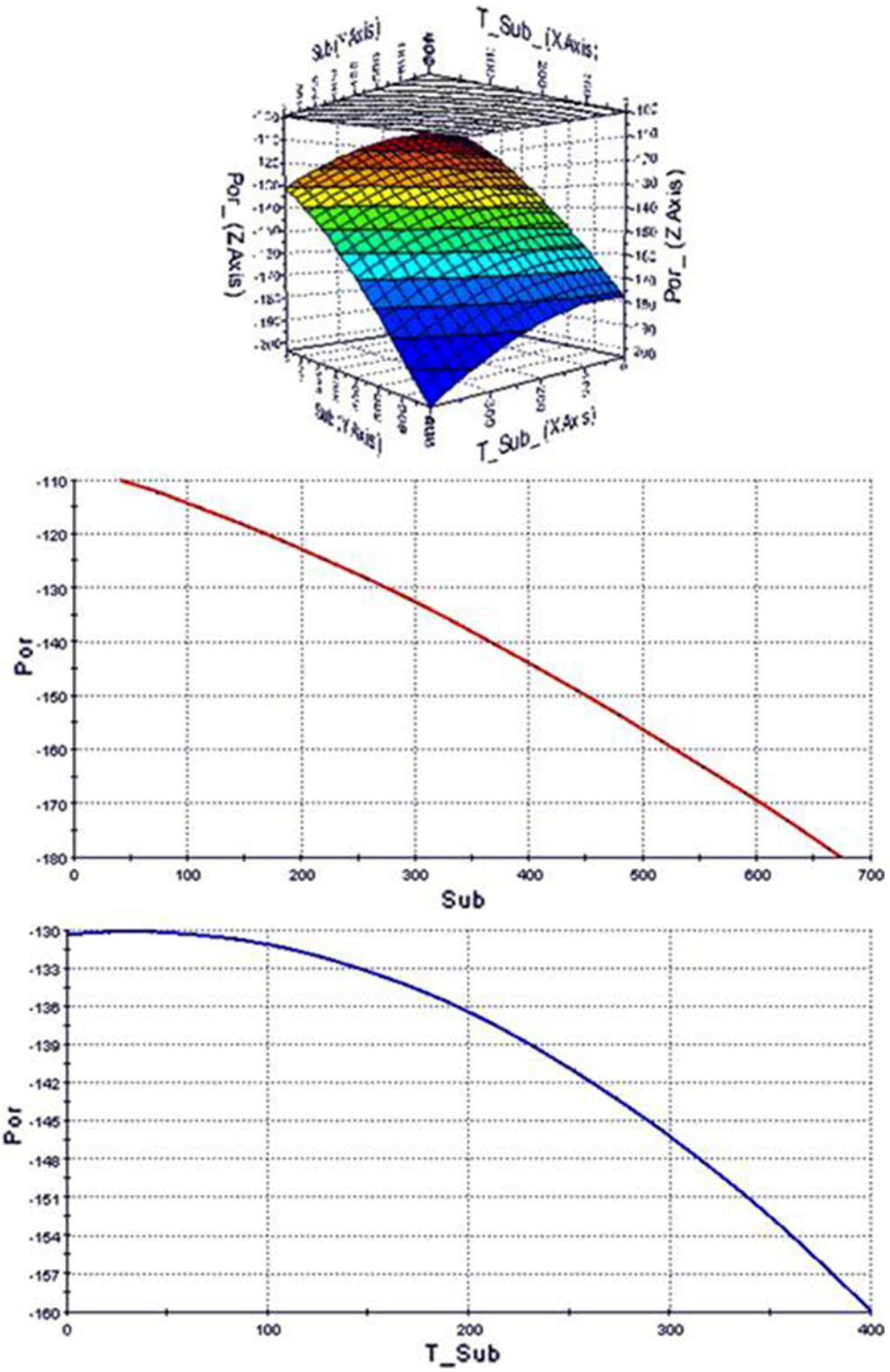

Fig. 16 Porosity vs. substrate hardness and substrate temperature (*T_Sub* is the substrate temperature; *Por_ is* the deposit porosity; *Sub* is the substrate hardness)

cold-sprayed particles, it is possible to obtain good quality deposits with lower temperatures and particles velocity levels. As the difference between the hardness of the substrate and the particles decreases, it is necessary to employ more severe conditions in terms of high pressure and high temperature. In general, the yield strength of the material affects the critical velocity required to induce adiabatic shear and therefore the ability of the material to form a strong, metallurgical bond. An interesting aspect is represented by the grain size variation as a function of processing parameters. The deposit grain size decreases with increasing pressure and increasing gas temperature (directly related to the increase of the particle speed). Such behavior is shown for Al particles deposited on AZ91 Mg alloy (Fig. 12).

In the present analysis, it is fundamental to employ the so called "scatter matrix" that allows the immediate recognition of how much the different variables are correlated to each other. Actually, the parameters are correlated strongly if the corresponding value in the table is distant from zero in a range between −1 and 1. If the value is 1, the parameters are directly proportional, while if the value is −1, the parameters are inversely proportional. An example of the present study is given in Table 1 from such a matrix, it is also possible to observe the different weight of all the parameters, the more the value differs from 0 the more it influences the corresponding variable.

By focusing the attention on the variation of the analyzed outputs, it is evident how the deposit microstructure is strongly influenced by the particle velocity which is directly related to gas temperature and pressure; then it is influenced by the gas density and by the starting particle dimension. The deposit microhardness is strongly related to the substrate microhardness, and, with the same weight, to the particle velocity and dimension. The adhesion strength is largely influenced by the particle velocity, by the substrate temperature, and by the particle dimensions. The deposit porosity is mainly dependent on the substrate temperature and hardness. Deposit microhardness and porosity, as a function of substrate microhardness and gas pressure dependence, is clearly shown in Fig. 13.

It is clear how deposit porosity increases with the increase of the substrate hardness up to a maximum and then it decreases with the increase of substrate hardness. The deposit hardness continuously increases as the substrate hardness increases. By analyzing in particular each single output as a function of the main input parameters influencing its behavior, we can see that the grain size is strongly influenced by the particle velocity which is directly related to the gas temperature and pressure, by the gas density, and by the starting particle dimension.

By correlating outputs with inputs through the use of modeFRONTIER, it is possible to achieve "phenomenological modeling," refine and calibrate the predictive models that simulate the phenomena in question ("Calibration") and validate these models ("Validation"). The methodological approach used was an empirical approach without pre-allocated analytical framework. The experimental data, appropriately filtered and reordered, are processed in order to build meta-models representative of the n-dimensional phenomenon and referring to an experimental database. The meta-model can be considered a black box capable of providing the desired output values of the variables following the introduction of the input variables. Through the use of the algorithm ED (evolutionary design), which provides with the output analytical expression, the equations simulating the processes have been obtained and validated. The advantage of this method is to use the very powerful numerical tools, which generate very complex forecasting models.

Taking a look at the results analyzed through modeFRONTIER, it is evident that adhesion strength increases with the increase of the particle velocity and decreasing of the substrate temperature (Fig. 14). The adhesion strength also increases with the increase of the gas temperature.

An interesting result is represented by the grain size behavior. Figure 15 shows how the deposit grain size decreases with the increasing of the particle velocity and the substrate hardness.

In Fig. 16, we see how the deposit porosity decreases as the substrate hardness and the substrate temperature increase.

How each fundamental mechanical or microstructural property of the deposits is governed by different processing parameters must be noted. In such scenario, it is possible to tune the processing parameters in order to optimize one of the analyzed mechanical or microstructural properties (and, at the same time, reduce the possibility of lower performances of the coatings caused by the worsening of other properties). A multiobjective optimization tool allows us to optimize one or more output parameters indicating which processing parameters should be tuned and also to individuate the ranges of modification inside the design space. Many examples can be underlined. Deposit porosity is strongly influenced by the substrate hardness and temperature so that by increasing the substrate hardness and the substrate temperature it is possible to decrease the deposit porosity. In such conditions, there is a very narrow range of possible particles velocity that can be employed to obtain a good quality deposit. If the adhesion strength is taken into account also, the range is further reduced. On the contrary, a deposit with low porosity but with a

Table 2 Output MSE cold spray

Output	MSE
Adhesion strength (MPa)	64.9
Microhardness (HV)	17.8
Porosity (%)	0.25
Grain size (nm)	729

Table 3 Adhesion strength error calculated for the six validation design

Adhesion strength				
	Numerical	Experimental	(Num-Exper)	(Num-Exper)2
Design 1	269	280	−10.9	119.7
Design 2	113.9	105	8.9	79.1
Design 3	68.5	60	8.5	72.1
Design 4	28.6	18	10.6	113.4
Design 5	10.6	10	0.65	0.42
Design 6	57.2	55	2.2	4.8
Mean square error				64.9

Table 5 Deposit porosity error calculated for the six validation design

Porosity				
	Numerical	Experimental	(Num-Exper)	(Num-Exper)2
Design 1	1.2	1.2	0.04	0.002
Design 2	12.2	13	−0.8	0.64
Design 3	0.18	0.2	−0.02	0.0004
Design 4	9.1	10	−0.9	0.8
Design 5	0.015	0.01	0.005	3.2E−05
Design 6	0.9	1.2	−0.3	0.09
Mean square error				0.25

low adhesion strength is obtained. An interesting situation is represented by the relationships between the adhesion strength and the deposit microhardness. They are related to the same input parameters but with an inverse proportionality. They are strongly influenced by gas pressure and temperature and obviously by particles velocity; but by tuning such input parameters, it was demonstrated that by increasing adhesion strength, a decrease in grain size is produced with a contemporary increase in mechanical properties. Another interesting analysis can be done on each single input parameter and by observing the effect on microstructural and mechanical behavior. All the output properties of the deposits are governed by the starting particles dimensions. The gas density has a strong influence on the deposit grain size and a minor effect on the remaining properties. Particle velocity appears to be the most influencing processing parameter. The substrate temperature appears to influence both adhesion strength and porosity while it has a lower effect on microhardness and grain size. The substrate hardness appears to strongly influence porosity, microhardness, and grain size while it has a lower influence on adhesion strength.

The analytical instrument used for the calculation of the error between output numerically and experimentally has been the mean square error (MSE) applied on the points of measurement of the specific size of output.

Expressing the discrepancy between experimental and numerical values as follows:

$$\Delta y_i = y_{\mathrm{exp},i} - y_{\mathrm{num},i} \tag{1}$$

the MSE for the outputs representative of a point is equal to:

$$\mathrm{MSE} = \sum_{i=1}^{6} \frac{(\Delta y_i)^2}{6} \tag{2}$$

Table 2 shows the MSE calculated on the outputs relating to the cold spray. To give them a physical sense, which is attributable to the units of measure of the question, was sufficient to calculate the square root.

As already mentioned, the results are a compromise between the minimal error and the fact that they are as representative as possible of the entire database. The errors calculated by modeFRONTIER for each validation design are shown in Tables 3, 4, 5, and 6.

An in-depth analysis of the calculated errors can lead to the conclusion that the developed model is really precise, also due to the large number of experimental conditions employed to develop the used database. Such a model can be used to

Table 4 Microhardness error calculated for the six validation design

Microhardness				
	Numerical	Experimental	(Num-Exper)	(Num-Exper)2
Design 1	340.8	335	5.8	33.9
Design 2	283.7	285	−1.3	1.74
Design 3	48.8	51	−2.16	4.67
Design 4	57.8	50	7.8	60.8
Design 5	170.4	170	0.4	0.16
Design 6	477.3	475	2.3	5.4
Mean square error				17.8

Table 6 Deposit grain size calculated for the six validation design

Grain size				
	Numerical	Experimental	(Num-Exper)	(Num-Exper)2
Design 1	27.3	28	−0.65	0.4
Design 2	18.6	20	−1.3	1.8
Design 3	79.3	75	4.3	18.3
Design 4	1,264.3	1,200	64.3	4,136.8
Design 5	39	35	4	16
Design 6	100.6	115	−14.3	206
Mean square error				729

optimize the properties of metal–metal cold spray deposits and to be used as a provisional instrument in the development of alternative and different deposition conditions.

5 Conclusions

In the present paper, a large number of experimental results of mechanical and microstructural properties of cold-sprayed deposits, obtained in a broad range of processing parameters for metal particles deposited on metal substrates, are described. The effect of particles size and material, gas pressure and temperature, particles velocity and substrate hardness on coating adhesion, microstructure, hardness, and porosity were underlined. Such analyses were performed for different particles materials (Ti and Ti–alloys, Al and Al–alloys, Mg, Ni and Ni–alloys, Cu) deposited on different substrates. The study allowed us to obtain a very broad experimental space capable of including all the possible processing conditions for the actual cold spray technology. The results were employed to build a database consisting of 376 experimental conditions. The results were analyzed through a multi-objective optimization software (modeFRONTIER) in order to develop a provisional model capable of simulating the deposit properties as a function of different processing parameters. The employed method was the RSM (response surface methodology). Such method allows us to simulate the actual process through the use of physical laws with appropriate calibrated coefficients. The different weight of the processing parameters affecting the mechanical and microstructural properties of the deposits was calculated. The robustness of the developed model has been demonstrated by the error calculation between the experimental results and the calculated ones. The number of experimental data and the described model has optimal potential to provide with a tool capable of predicting coatings quality in very different experimental conditions.

References

1. Goldbaum D, Ajaja J, Chromik RR, Wong W, Yue S, Irissou E, Legoux JG (2011) Mechanical behavior of Ti cold spray coatings determined by a multi-scale indentation method. Mater Sci Eng A530:253–265
2. Goldbaum D, Shockley JM, Chromik RR, Rezaeian A, Yue S, Legoux JG, Irissou E (2011) The effect of deposition conditions on adhesion strength of ti and ti6al4v cold spray splats. J Therm Spray Technol. doi:10.1007/s11666-011-9720-3
3. Goldbaum D, Chromik RR, Yue S, Irissou E, Legoux JG (2011) Mechanical property mapping of cold sprayed Ti splats and coatings. J Therm Spray Technol 20(3):486–496
4. Kim K, Kuroda S, Watanabe M, Huang R, Fukanuma H, Katanoda H (2011) Comparison of oxidation and microstructure of warm-sprayed and cold-sprayed titanium coatings. J Therm Spray Technol. doi:10.1007/s11666-011-9703-4
5. Hussain T, McCartney DG, Shipway PH (2011) Impact phenomena in cold-spraying of titanium onto various ferrous alloys. Surf Coat Tech 205:5021–5027
6. Cinca N, Barbosa M, Dosta S, Guilemany JM (2010) Study of Ti deposition onto Al alloy by cold gas spraying. Surf Coat Tech 205: 1096–1102
7. Moy CKS, Cairney J, Ranzi G, Jahedi M, Ringer SP (2010) Investigating the microstructure and composition of cold gas-dynamic spray (CGDS) Ti powder deposited on Al 6063 substrate. Surf Coat Tech 204:3739–3749
8. Christoulis DK, Guetta S, Guipont V, Jeandin M (2011) The influence of the substrate on the deposition of cold-sprayed titanium: an experimental and numerical study. J Therm Spray Technol 20(3): 523–533
9. Berube´ G, Yandouzi M, Zuniga A, Ajdelsztajn L, Villafuerte J, Jodoin B (2011) Phase stability of Al-5Fe-V-Si coatings produced by cold gas dynamic spray process using rapidly solidified feedstock materials. J Therm Spray Technol. doi:10.1007/s11666-011-9716-z
10. Bu H, Yandouzi M, Lu C, Jodoin B (2010) Effect of heat treatment on the intermetallic layer of cold sprayed aluminum coatings on magnesium alloy. Surf Coat Technol 205:4665–4671
11. Tao Y, Xiong T, Sun C, Kong L, Cui X, Li T, Song GL (2010) Microstructure and corrosion performance of a cold sprayed aluminium coating on AZ91D magnesium alloy. Corr Sci 52:3191–3197
12. Wang Q, Birbilis N, Zhang MX (2011) Interfacial structure between particles in an aluminum deposit produced by cold spray. Mater Lett 65:1576–1578
13. Luzin V, Spencer K, Zhang MX (2011) Residual stress and thermo-mechanical properties of cold spray metal coatings. Acta Mater 59: 1259–1270
14. Champagne VK, Helfritch DJ, Trexler MD, Gabriel BM (2010) The effect of cold spray impact velocity on deposit hardness. Model Simul Mater Sci Eng 18:1–8
15. Lee H, Shin H, Ko K (2010) Effects of gas pressure of cold spray on the formation of Al-based intermetallic compound. J Therm Spray Technol 19(1–2):102–109
16. King PC, Jahedi M (2010) Relationship between particle size and deformation in the cold spray process. Appl Surf Sci 256:1735–1738
17. Zhang YY, Zhang JS (2011) Recrystallization in the particles interfacial region of the cold-sprayed aluminum coating: strain-induced boundary migration. Mater Lett 65:1856–1858
18. Richer P, Jodoin B, Ajdelsztajn L, Lavernia EJ (2006) Substrate roughness and thickness effects on cold spray nanocrystalline Al-Mg coatings. J Therm Spray Technol 15(2):246–254
19. Rech S, Trentin A, Vezzu` S, Legoux JG, Irissou E, Guagliano M (2011) Influence of pre-heated Al 6061 substrate temperature on the residual stresses of multipass Al coatings deposited by cold spray. J Therm Spray Technol 20(1-2):243–251
20. Hall AC, Brewer LN, Roemer TJ (2008) Preparation of aluminum coatings containing homogenous nanocrystalline microstructures using the cold spray process. J Therm Spray Technol 17(3):352–359
21. Kang K, Park H, Bae G, Lee C (2012) Microstructure and texture of Al coating during kinetic spraying and heat treatment. J Mater Sci. doi:10.1007/s10853-012-6259-8
22. DeForce BS, Eden TJ, Potter JK (2011) Cold spray Al-5 % Mg coatings for the corrosion protection of magnesium alloys. J Therm Spray Technol 20(6):1352–1358
23. Spencer K, Zhang MX (2011) Optimisation of stainless steel cold spray coatings using mixed particle size distributions. Surf Coat Tech 205:5135–5140
24. Bala N, Singh H, Prakash S, Karthikeyan J (2012) Investigations on the behavior of HVOF and cold sprayed Ni-20Cr coating on T22 boiler steel in actual boiler environment. J Therm Spray Technol 21(1):144–158

25. Bala N, Singh H, Prakash S, Karthikeyan J (2011) Characterization and high-temperature oxidation behavior of cold-sprayed Ni-20Cr and Ni-50Cr coatings on boiler steels. Met Mat Trans 42A:3399–3416
26. Spencer K, Luzin V, Matthews N, Zhang MX (2012) Residual stresses in cold spray Al coatings: the effect of alloying and of process parameters. Surf Coat Technol 206:4249–4255
27. Bu H, Yandouzi M, Lu C, MacDonald D, Jodoin B (2012) Cold spray blended Al+Mg17Al12 coating for corrosion protection of AZ91D magnesium alloy. Surf Coat Tech 207:155–162
28. Xiong Y, Xiong X, Yoon S, Bae G, Lee C (2011) Dependence of bonding mechanisms of cold sprayed coatings on strain-rate-induced non-equilibrium phase transformation. J Therm Spray Technol 20(4): 860–865
29. Kalkhoran SM, Choi WB, Gouldstone A (2012) Estimation of plastic anisotropy in Ni–5% Al coatings via spherical indentation. Acta Mater 60:803–810
30. Xiong Y, Bae G, Xiong X, Lee C (2010) The effects of successive impacts and cold welds on the deposition onset of cold spray coatings. J Therm Spray Techno 19(3):575–585
31. Bae G, Jang J, Lee C (2012) Correlation of particle impact conditions with bonding, nanocrystal formation and mechanical properties in kinetic sprayed nickel. Acta Mater 60:3524–3535
32. Jin YM, Cho JH, Park DY, Kim JH, Lee KA (2011) Manufacturing and macroscopic properties of cold sprayed Cu-In coating material for sputtering target. J Therm Spray Technol 20(3):497–507
33. Seo D, Ogawa K, Sakaguchi K, Miyamoto N, Tsuzuki Y (2012) Parameter study influencing thermal conductivity of annealed pure copper coatings deposited by selective cold spray processes. Surf Coat Tech 206:2316–2324
34. Eason PD, Fewkes JA, Kennett SC, Eden TJ, Tello K, Kaufman MJ, Tiryakioglu M (2011) On the characterization of bulk copper produced by cold gas dynamic spray processing in as fabricated and annealed conditions. Mater Sci Eng A528:8174–8178
35. Li WY, Li CJ, Liao H (2010) Significant influence of particle surface oxidation on deposition efficiency, interface microstructure and adhesive strength of cold-sprayed copper coatings. Appl Surf Sci 256: 4953–4958
36. Huang R, Fukanuma H (2011) Study of the influence of particle velocity on adhesive strength of cold spray deposits. J Therm Spray Technol. doi:10.1007/s11666-011-9707-0
37. Meng X, Zhang J, Zhao J, Liang Y, Zhang Y (2011) Influence of gas temperature on microstructure and properties of cold spray 304SS coating. J Mater Sci Tech 27(9):809–815
38. Sundararajan G, Chavan NM, Sivakumar G, Phani PS (2010) Evaluation of parameters for assessment of inter-splat bond strength in cold-sprayed coatings. J Therm Spray Technol 19(6): 1255–1266
39. Grujicic M, Zhao CL, DeRosset WS, Helfritch D (2004) Adiabatic shear instability based mechanism for particle/substrate bonding in the cold-gas dynamic-spray process". Mater Des 25:681–688
40. Grujicic M, Saylor JR, Beasley DE, DeRosset WS, Helfritch D (2003) Computational analysis of the interfacial bonding between feed powder particles and the substrate in the cold-gas dynamic-spray process. Appl Surf Sci 219:211–327
41. Trinchi A, Yang YS, Tulloh A, Zahiri SH, Jahedi M (2011) Copper surface coatings formed by the cold spray process: simulations based on empirical and phenomenological data. J Therm Spray Technol 20(5):986–991